Rare Met. (2017) 36(3):209–219
DOI 10.1007/s12598-015-0564-8

RARE METALS
www.editorialmanager.com/rmet

Empirical model to predict mass gain of cobalt electroless deposition on ceramic particles using response surface methodology

Akbar Heidarzadeh, Reza Taherzadeh Mousavian, Rasoul Azari Khosroshahi*, Yalda A. Afkham, Hesam Pouraliakbar

Received: 12 January 2015 / Revised: 11 May 2015 / Accepted: 7 July 2015 / Published online: 1 August 2015

Abstract This investigation was undertaken to predict the mass gain (MG) of cobalt electroless deposition (ED) on ceramic SiC particles. Response surface methodology (RSM) based on a full factorial design with three ED parameters and 30 runs was used to conduct the experiments and to establish a mathematical model by means of Design-Expert software. Three ED parameters considered were pH, bath temperature and ceramic particle morphology. Analysis of variance was applied to validate the predicted model. The results of confirmation analysis by scanning electron microscopy (SEM) show that the developed models are reasonably accurate. The pH is the most effective parameter for the MG. Also, the highest mass gain is obtained for the lowest pH, highest bath temperatures and heat-treated SiC particles. In addition, the developed model shows that the optimal parameters to get a maximum value of mass gain are pH, bath temperature and ceramic particle state of 8, 70 °C and heat treatment, respectively.

Keywords Electroless deposition; Cobalt; SiC particles; Mathematical model; Response surface method

A. Heidarzadeh
Faculty of Engineering, Azarbaijan Shahid Madani University, Tabriz 7200-000, Iran

R. T. Mousavian, R. A. Khosroshahi*, Y. A. Afkham
Department of Materials Engineering, Sahand University of Technology, Tabriz 65175-4171, Iran
e-mail: rakhosroshahi@gmail.com

H. Pouraliakbar
Department of Advanced Materials, WorldTech Scientific Research Center (WT-SRC), Tehran 71857-3834, Iran

1 Introduction

Aluminum metal matrix composites (MMCs) are the most significant materials in aerospace and automotive industries due to their superior mechanical properties [1–11]. A variety of methods have been used for synthesizing these composites, but the liquid-state route is the simplest technique with lower cost [1–5]. However, low wettability of ceramic particles as reinforcement by liquid metal matrix is a major problem in fabrication of MMCs via casting (liquid-state) method. This important challenge is addressed by the use of metal-coated ceramic particles and the addition of reactive metals like Mg to increase the wettability of the composites [12]. Metallic coating of ceramic powder particulates is commonly performed in order to alter the specific properties of ceramics. The mass gain (MG, %) of coated metal on ceramic particle plays an important role in this regard. Copper, nickel and cobalt are three important metals, which were reported for fabrication of metal-coated ceramic particles as reinforcements of MMCs [13–21].

Electroless deposition (ED) is one of the liquid preparation routes, and it is widely used for preparing metallic coatings onto various surfaces. It provides a mean for metallic coating of ceramic reinforcement without the requirement for costly electrolytic bath or other electroplating equipment and associated electrical running costs. Also, ED is proved to controllably provide homogenous thickness coatings on complex-shaped components [22–24].

MG is generally influenced by ED parameters such as pH, bath temperature and ceramic particle morphology, which should be optimized. Response surface methodology (RSM) invented by Box and Wilson [25] in 1951 and developed by Box and Hunter [26] was employed to model and optimize the different metallurgical processes [27–35],

which has two key goals. The first one is optimizing the responses, which are a function of different process input parameters. The second one is developing the mathematical models between the input parameters and the determined responses. The RSM steps for modeling and prediction of MG during ED can be summarized as follows: identifying ED parameters which have effects on MG; considering a practical restrictions of the identified parameters; establishing a preferred experimental design; conducting the tests in accordance with the established experimental design; measuring MG for each of the tests; developing the mathematical models; controlling the model sufficiency by means of analysis of variance (ANOVA); and discovering the effect of the parameters on MG and optimizing them.

Recently, some investigators have used RSM to predict or optimize some of the coating processes for different metals and alloys [36–39]. Oraon et al. [36, 37] used RSM to predict the electroless Ni and Ni–B on a pure copper substrate. In their studies, a second-order response surface model with central composite design (CCD) was used. They showed that reducing agent, source of metal and temperature significantly affect the deposition. Poroch-Seritan et al. [38] used CCD and RSM methods for modeling of nickel electroplating process. Optimum conditions of current density, temperature and pH were obtained in their study. Choudhury et al. [39] used RSM to identify the influencing process parameters of Ni–P ED coating on a pure copper substrate. In their study, deposited contents of nickel and phosphorus in Ni–P coatings were evaluated by energy-dispersive X-ray (EDX) analysis, and these contents were considered as response variables for statistical analysis.

Even though the prior investigators [36–39] explored mathematical models in the case of some metals and alloys, a research into establishing mathematical relationships between the process parameters and MG of deposited cobalt on ceramic particles is lacking. Therefore, the aim of this study is to apply RSM in conjunction with full factorial design and to establish the functional relationships between ED parameters (i.e., pH, bath temperature and ceramic particle morphology) and response of MG.

2 Experimental

2.1 Design of experiments

In this investigation, full factorial design was used for design of experiments. For this purpose, design matrix including 30 runs and three parameters (pH, at five levels; bath temperature, at three levels; and SiC particle morphology, at two levels) was employed. The levels and actual values of the parameters are given in Table 1. Also, the measured response was MG of deposited cobalt on SiC ceramic particles. Moreover, Design-Expert version 8.0 software was used for preparing the experimental design, which is presented in Table 2.

Table 1 Coded and actual values of parameters

Levels	pH (*A*)	Temperature (*B*)/°C	SiC morphology (*C*)
−1.0	8.0	50	As received
−0.5	8.5	–	–
0	9.0	60	–
0.5	9.5	–	–
1.0	10.0	70	Heat treated

Table 2 Design layout including experimental (Exp.) and predicted values (Pre.)

Samples	Run	Parameters			MG/%		
		A	*B*/°C	*C*	Exp.	Pre.	Error
1	9	8.0	50	As received	58.96	57.67	−2.19
2	21	8.5			55.09	53.09	−3.63
3	10	9.0			51.30	49.75	−3.02
4	3	9.5			47.03	47.66	1.34
5	2	10.0			45.60	46.82	2.68
6	28	8.0	60		61.50	67.26	9.37
7	24	8.5			56.80	60.60	6.69
8	20	9.0			53.10	54.18	2.03
9	23	9.5			51.20	49.01	−4.28
10	22	10.0			48.60	45.08	−7.24
11	17	8.0	70		88.01	85.43	−2.93
12	13	8.5			82.10	74.69	−9.03
13	29	9.0			62.10	65.20	4.99
14	7	9.5			55.50	56.95	2.61
15	15	10.0			47.50	49.94	5.14
16	5	8.0	50	Heat treated	71.20	69.85	−1.90
17	12	8.5			67.80	65.20	−3.83
18	8	9.0			62.10	61.79	−0.50
19	26	9.5			56.80	59.62	4.96
20	25	10.0			54.30	58.70	8.10
21	4	8.0	60		75.04	79.12	5.44
22	19	8.5			70.86	71.38	0.73
23	16	9.0			67.03	64.89	−3.19
24	14	9.5			62.61	59.64	−4.74
25	11	10.0			61.11	55.64	−8.95
26	30	8.0	70		96.03	94.97	−1.10
27	1	8.5			88.40	84.16	−4.80
28	18	9.0			66.60	73.12	9.79
29	6	9.5			65.03	66.25	1.88
30	27	10.0			60.12	59.17	−1.58

2.2 ED coating and experimental details

The SiC powders used in this study were in two forms: (1) 99.5 % purity with an average particle size of 80 μm; (2) the second kind of SiC powders were prepared from the heat treatment at 800 °C for 2 h. Figure 1 shows the morphology of the two kinds of SiC powder forms used in this study. As it can be seen from Fig. 1a, as-received SiC powders have sharp edges and almost smooth surfaces. Figure 1b shows the morphology of SiC powders heated in air atmosphere. As it can be seen, a porous oxide layer forms in some parts of the powders (yellow rectangles in Fig. 1b), which might affect the mechanism of cobalt deposition.

The first step was cleaning the SiC powders using HF solution to remove impurities from the surface. Figure 2 shows the flowchart of cobalt coating procedures. According to Fig. 2, the powders were pretreated in three steps followed by progressive drying and ED. Table 3 shows the details of the chemicals used for pretreatment of

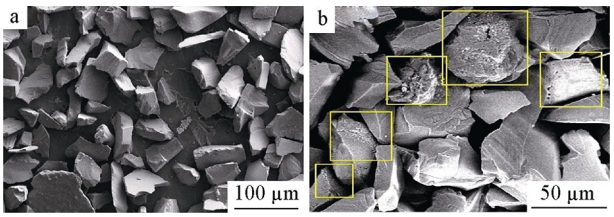

Fig. 1 SEM images of as-received powders with an average particle size of 80 μm **a** and heat-treated SiC powders at 800 °C for 2 h **b**

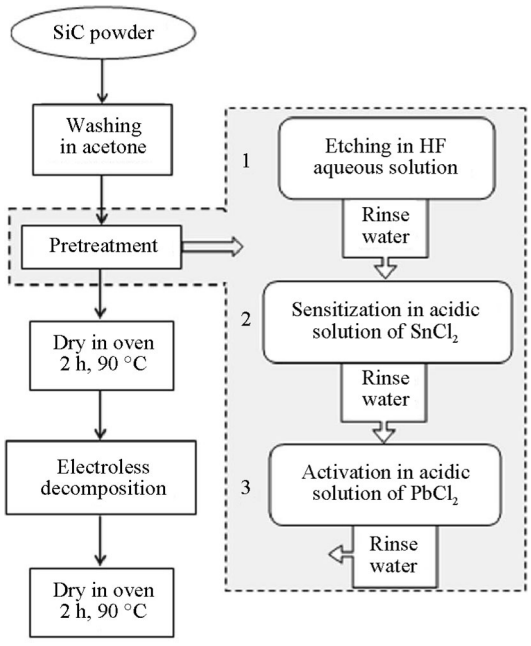

Fig. 2 Flowchart of preparation procedure of ED for cobalt

Table 3 Details of SiC powder pretreatment and chemicals used in Fig. 2. Washing in distilled water for several times in coarsening, sensitization and activation processes

Treatments	Composition	Concentration	Time/min	*T*/°C
Washing	Acetone (100 ml)	–	10	–
Coarsening	HF (40 %)	100.0 ml·L^{-1}	10	25
	NaF	2 g·L^{-1}		
Sensitization	$SnCl_2$	10 g·L^{-1}	15	25
	HCl (37 %)	0.50 ml·L^{-1}		
Activation	$PdCl_2$	0.05 g·L^{-1}	15	25
	HCl (37 %)	0.10 ml·L^{-1}		

Table 4 Composition of bath used for ED of cobalt coating on SiC particles

Roles in bath	Composition	Concentration/(g·L^{-1})
Main salt	$CoSO_4{\cdot}7H_2O$	25.0
Reducing agent	$NaH_2PO_2{\cdot}H_2O$	25.0
Complexion agent	$C_6H_5Na_3O_7{\cdot}2H_2O$	50.0
Buffering agent	H_3BO_3	25.0
pH adjuster	NaOH	–
SiC powder	–	2.5

SiC powders, showing that all three steps were done at room temperature followed by drying at 90 °C for 1 h. The composition of Co ED bath is given in Table 4, showing the composition and concentration of the materials used for the bath. All the procedures were carried out with the magnetic stirring speed of 400 r·min^{-1}.

In this study, MG was calculated as the response of mathematical modeling in accordance with Eq. (1):

$$\mathrm{MG} = \left(\frac{W_\mathrm{f} - W_\mathrm{i}}{W_\mathrm{m}}\right) \times 100\,\% \tag{1}$$

where W_f is the weight of coated SiC powders, W_i is initial weight of SiC powders, and W_m is the weight of cobalt in the bath that could deposit on the particles.

Microstructural and elemental investigations of the particles before and after coating treatment were performed using two kinds of scanning electron microscopes (SEM, Cam Scan Mv2300) equipped with energy-dispersive spectroscopy (EDS) and SEM (KYKY-EM3200).

2.3 Establishing mathematical model

The mathematical models were established using a second-order polynomial regression model including the main and interaction influences of the parameters. If the measured response (*Y*), i.e., MG of the ED coating, is a function of parameters, i.e., pH (*A*), bath temperature (*B*) and SiC particle morphology (*C*), the response surface can be

explored as Eq. (1). As well, the employed regression equation in this study is presented as Eq. (2):

$$Y = f(A, B, C) \tag{2}$$

$$Y = b_0 + \sum_{i=1}^{k} b_i k_i + \sum_{i=1}^{k} b_{ii} X_i^2 + \sum_{i<j} b_{ij} X_i X_j \tag{3}$$

where Y is the measured response, X_i and X_j are the independent variables, b_0 stands for the mean value of responses, and b_i, b_{ii} and b_{ij} are linear, quadratic and interaction constant coefficients, correspondingly. In addition, the coefficients of Eq. (3) can be computed using Eqs. (4)–(7) [40, 41]:

$$b_0 = 0.142857\left(\sum Y\right) - 0.035714 \sum \sum (X_{ii} Y) \tag{4}$$

$$b_i = 0.041667\left(\sum X_i Y\right) \tag{5}$$

$$b_{ii} = 0.03125 \sum (X_{ii} Y) + 0.00372 \sum \sum (X_{ii} Y) - 0.035714\left(\sum Y\right) \tag{6}$$

$$b_{ij} = 0.0625 \sum \left(X_{ij} Y\right) \tag{7}$$

where X_{ii} and X_{ij} are quadratic and interaction of the variables. The selected polynomials considering the three ED parameters (A, B and C) are presented as Eq. (8). Furthermore, the Design-Expert software at 95 % confidence level was employed in order to compute the coefficients of the models. Moreover, the sufficiency of the models was confirmed using ANOVA, and the models were illustrated by contour and 3D plots.

$$Y = b_0 + b_1(A) + b_2(B) + b_3(C) + b_{11}(A^2) + b_{22}(B^2) + b_{33}(C^2) + b_{12}(AB) + b_{13}(AC) + b_{23}(BC) \tag{8}$$

3 Results and discussion

3.1 Numerical relationships and ANOVA

The fraction of design space (FDS) graph is illustrated in Fig. 3. This graph is a line graph showing the relationship between the volume of the design space (area of interest) and amount of prediction error. The curve indicates that the design space fraction has a given prediction error or lower. In general, a lower (approximately 1.0 or lower) and flatter FDS curve is better, and lower is more important than flatter. Moreover, the standard (Std) error of design graph is depicted in Fig. 4. This graph is a contour (Fig. 4a) or

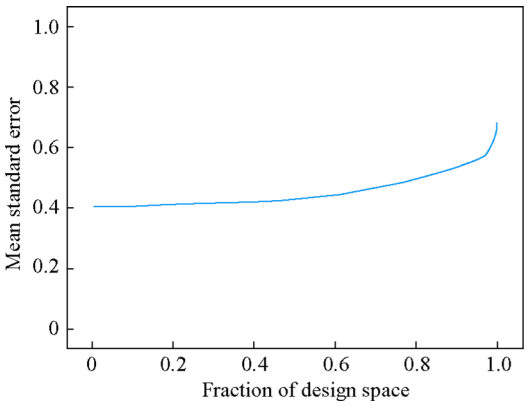

Fig. 3 FDS graph of developed design matrix

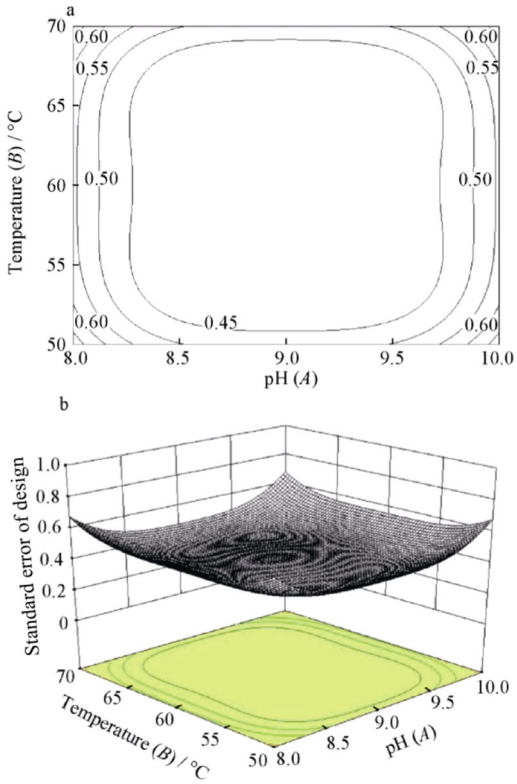

Fig. 4 Standard error of design graph: **a** contour plot and **b** 3D plot

3D (Fig. 4b) plot showing the standard error of prediction for areas in the design space. By default, these values are reflection of the design only, not of the response data. Generally, it is better for this graph to have relatively low standard error across the region of interest, which means approximately 1.0 or lower.

The total numerical relationship between the considered parameters and the response MG was achieved as follows:

$$MG_{total} = 59.54 - 11.66A + 7.06B + 5.35C - 6.16AB - 0.077AC - 0.66BC + 2.49A^2 + 3.29B^2 \quad (9)$$

Also, the mathematical models for each of the SiC particle morphologies were developed as follows:

$$MG_{As\ received} = 99.55 - 19.41A + 2.37B - 6.16AB + 2.49A^2 + 0.033B^2 \quad (10)$$

$$MG_{Heat\ treated} = 119.59 - 19.56A + 2.23B - 0.62AB + 2.49A^2 + 0.033B^2 \quad (11)$$

Equations (9)–(11) predict MG of ED coatings. The normal plot of residuals, the predicted versus actual response plot, the residuals versus the predicted response plot and the residuals versus the experimental run plot are, respectively, illustrated in Fig. 5a–d, for the response MG. The normal probability plot indicates whether the residuals follow a normal distribution, in which case the points will follow a straight line. Figure 5a demonstrates that errors are extended normally because the residuals follow a straight line. Figure 5b reveals that the predicted response values are in good agreement with the actual ones within the ranges of the process parameters, because the data points are split evenly by the 45° line. Figure 5c and d reveals that numerical models predict the responses adequately due to randomly scattered residuals.

The ANOVA result for response MG is summarized in Table 5. The F value, P value, R^2 and adjusted R^2 are used for identifying the significance of the model and coefficients. Larger F value, R^2 and adjusted R^2, and smaller P value reveal that the model or a coefficient is significant. According to Table 5, the F value, P value, R^2 and adjusted R^2 for the predicted model are 33.03, <0.0001, 0.9264 and 0.8983, respectively. Therefore, it can be concluded that the predicted models are very adequate and significant. Also, from the error shown in Table 2, it is obvious that the developed model can predict the MG within ±10 % their experimental values. The error was calculated as follows:

$$\text{Error} = \frac{\text{Predicted} - \text{Experimental}}{\text{Experimental}} \times 100\,\% \quad (12)$$

Additionally, P values <0.05 verify that the coefficients are significant and P values >0.10 mean that the coefficients are not significant. Thus, according to the P

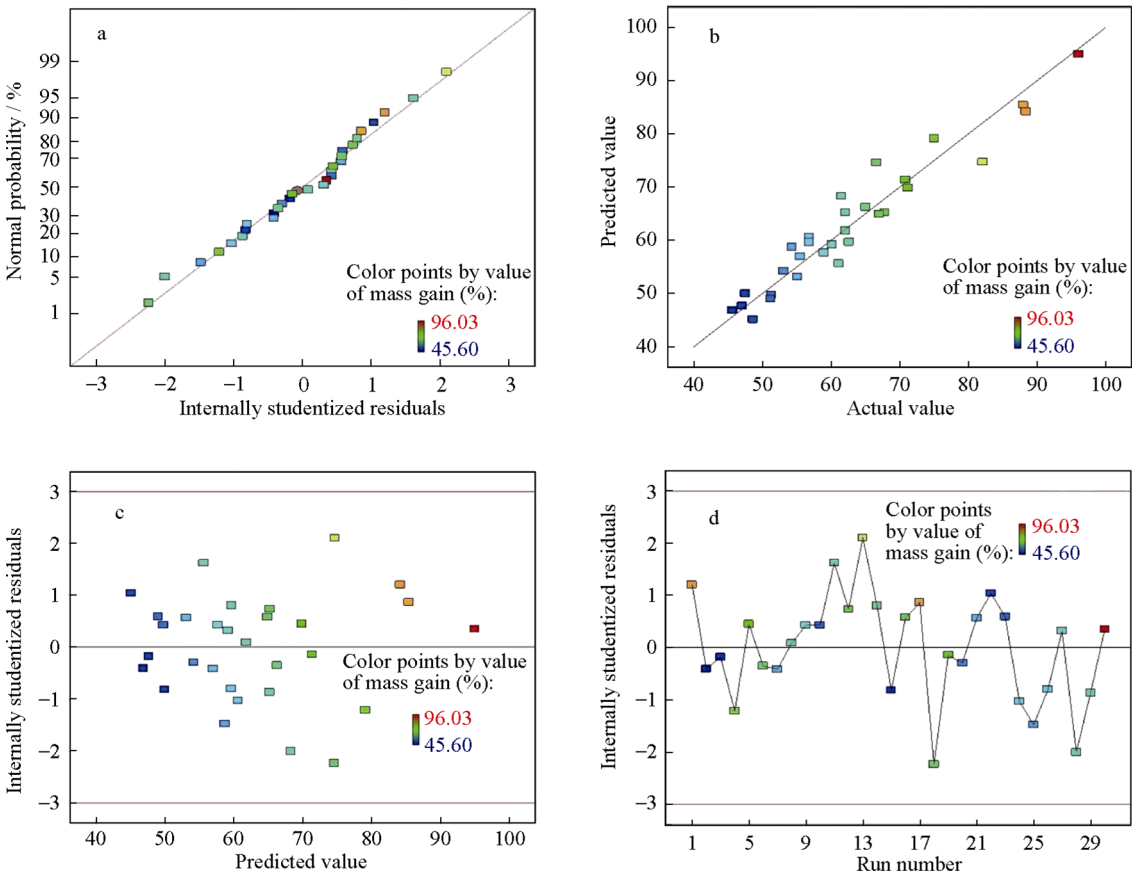

Fig. 5 Normal probability plot of residuals **a**, predicted versus actual response plot **b**, residuals versus predicted response plot **c**, and residuals versus experimental run plot **d** for MG

Table 5 ANOVA table for response MG

Source	Sum of squares	Degree of freedom	Mean square	*F* value	*P* value	Condition
Model	4391.020	8	548.880	33.030	<0.0001	Significant
A	2040.500	1	2040.500	122.810	<0.0001	
B	997.010	1	997.010	60.010	<0.0001	
C	860.170	1	860.170	51.770	<0.0001	
AB	379.640	1	379.640	22.850	0.0001	
AC	0.088	1	0.088	0.005	0.9426	
BC	8.780	1	8.780	0.530	0.4753	
A^2	32.510	1	32.510	1.960	0.1764	
B^2	72.310	1	72.310	4.350	0.0493	
Residual	348.910	21	16.610			
R^2	0.9264					
Adjusted R^2	0.8983					

F value, test for comparing model variance with residual (error) variance; *P* value, probability of seeing observed *F* value if null hypothesis is true; R^2, multiple correlation coefficient

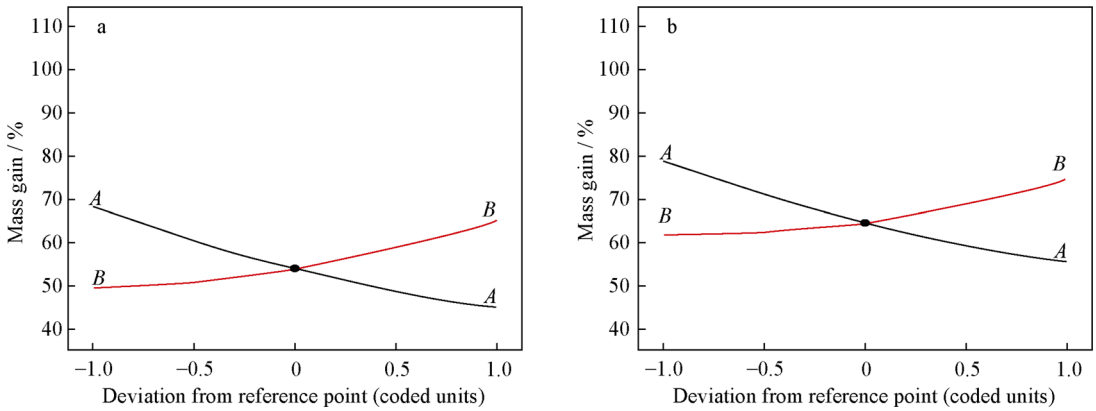

Fig. 6 Perturbation plot illustrating influence of ED parameters on MG for as-received **a** and heat-treated SiC particles **b**

values, *A*, *B*, *C*, *AB* and B^2 are significant terms for predicted model. After the reduction of the model by considering only the significant terms, the following mathematical model is achieved:

$$\mathrm{MG} = 60.79 - 11.66A + 7.06B + 5.35C - 6.16AB + 3.29B^2 \quad (13)$$

Furthermore, the *F* values prove that the orders of the significant terms in the model are as follows: $A > B > C > AB > B^2$.

3.2 Effect of parameters on MG

The perturbation plots of the response MG for the as-received and heat-treated SiC particles are presented in Fig. 6. This type of plots provides silhouette views of the response surface. It shows the change of the response MG when each parameter moves from the reference point, with all other parameters held constant at the reference value. Design-Expert software sets the reference point default at the middle of the design space (the coded 0 level of each parameter). The real benefit of this plot lies in when selecting the most effective parameters on response surfaces. The perturbation plots indicate that the parameter pH is somewhat more effective than parameter temperature for both types of SiC particles. Also, Fig. 7a–d shows the contour and 3D surface plots. These plots illustrate the interaction effect of any two parameters on the response when the other parameter is on its level zero (center level). According to Figs. 6 and 7, three important results can be obtained. First, the heat-treated SiC particles have higher MG compared with the as-received particles. Second, with the increase of pH, the MG of both as-received and heat-treated SiC particles decreases continuously. Third, higher bath temperatures cause higher MG in the case of both types of the particles.

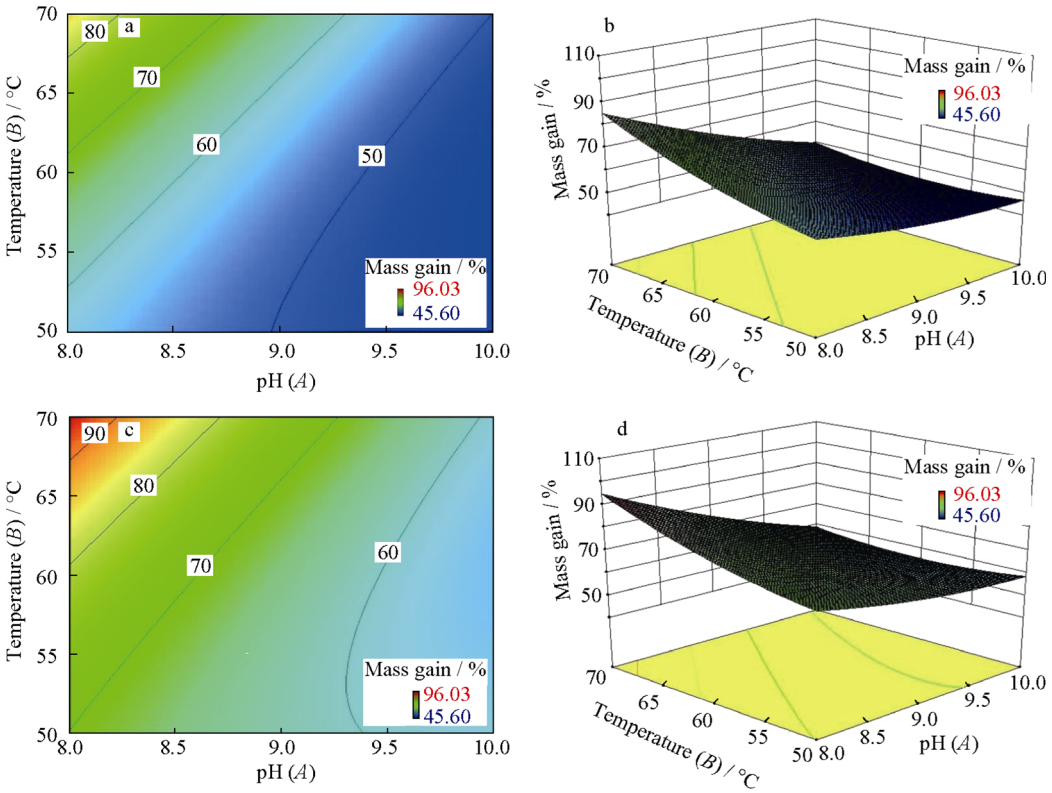

Fig. 7 Contour and 3D plots of response MG for **a**, **b** as-received and **c**, **d** heat-treated SiC particles

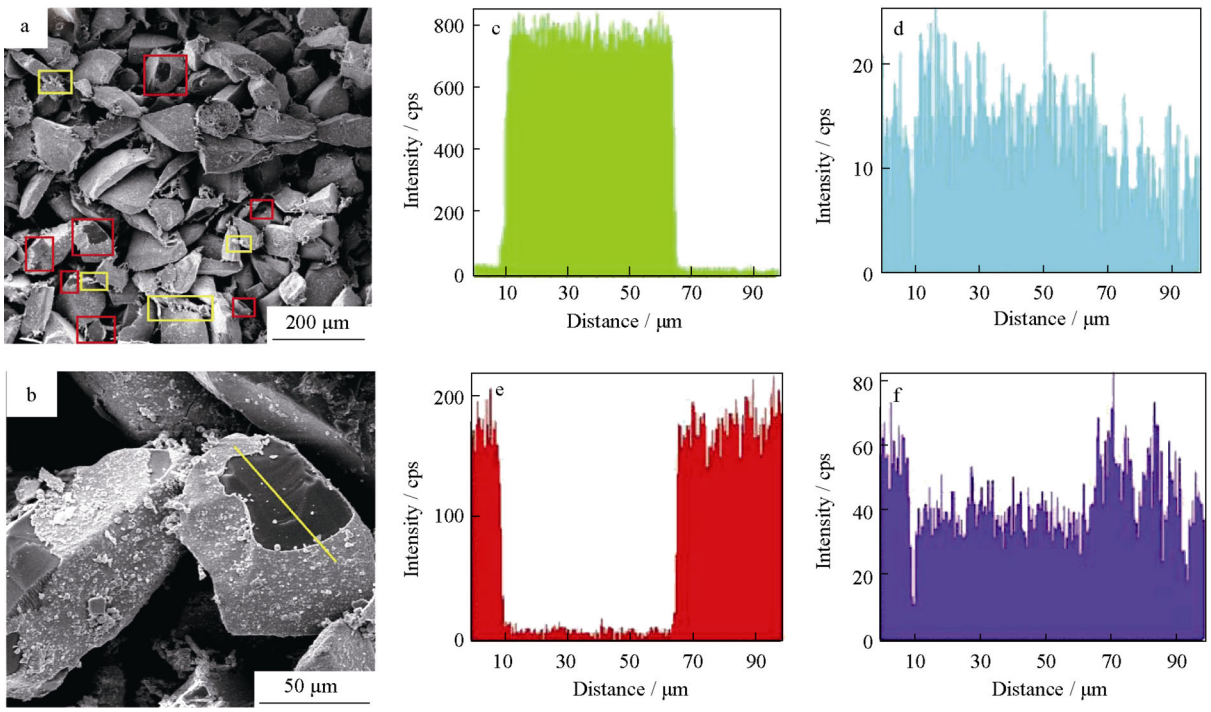

Fig. 8 SEM images **a**, **b** and corresponding EDS line scanning analysis of Sample 13: **c** Si, **d** C, **e** Mo and **f** P

In order to study the effect of ceramic particle morphology, pH and bath temperature on the morphology of coated particles, Samples 13, 18, 26 and 28 (Table 2) were selected for SEM characterizations. Figure 8 shows the morphology of Sample 13, in which as-received powders were coated by cobalt layer. Although yellow-colored rectangles show the formation of cobalt-free clusters, some uncoated parts are revealed after ED process in red-colored rectangles. Higher magnification SEM image and its line EDS analysis confirm that red-colored rectangles represent the places where poor traces of cobalt and phosphorous are detected. Figure 9 shows the morphology of Sample 28 related to a heat-treated sample which was coated by cobalt at pH of 9 and bath temperature of 70 °C. It also indicates the presence of uncoated parts (red-colored rectangles) and formation of cobalt-free clusters (yellow-colored rectangles), showing that in the ranges of pH and bath temperature, the morphology of ceramic particles might not be effective in the efficiency and MG of coating. Figure 9 clearly shows that cobalt layer was settled on the oxide layers (yellow-colored arrows in Fig. 9b, as justified by point EDS).

Figure 10 is related to a heat-treated sample that was coated by cobalt at optimized pH of 8 and bath temperature of 70 °C (Sample 26). In fact, the intensive effect of pH on cobalt coating could be understood by comparing the morphologies in Figs. 9 and 10. As can be observed, no uncoated parts could be seen in this morphology and point EDS analysis shows the detection of about 7.5 at% silicon element, indicating that the thickness of cobalt layer might be high enough for detection of low silicon content. In order to study the effect of bath temperature, Sample 18 (heat-treated powders, pH = 9 and bath temperature = 50 °C) was characterized by SEM to compare its morphology with that of Sample 28 (Fig. 9). This morphology indicates that a relatively considerable change would be obtained in the coating characteristics when a 20 °C reduction in bath temperature was conducted for heat-treated powders. The number of uncoated parts in the morphology of Sample 18 (red-colored rectangles in Fig. 11) is higher than that of Sample 28 (Fig. 9), showing that higher values of bath temperature seem to be more suitable for cobalt coating.

Based on the examinations, there is a relationship between the values of deposition time and MG, meaning that by decreasing the deposition time, a lower amount of cobalt will be deposited on the SiC powder surfaces. Jiang et al. [42] reported the main reactions that take place during cobalt deposition when hypophosphite is used as the

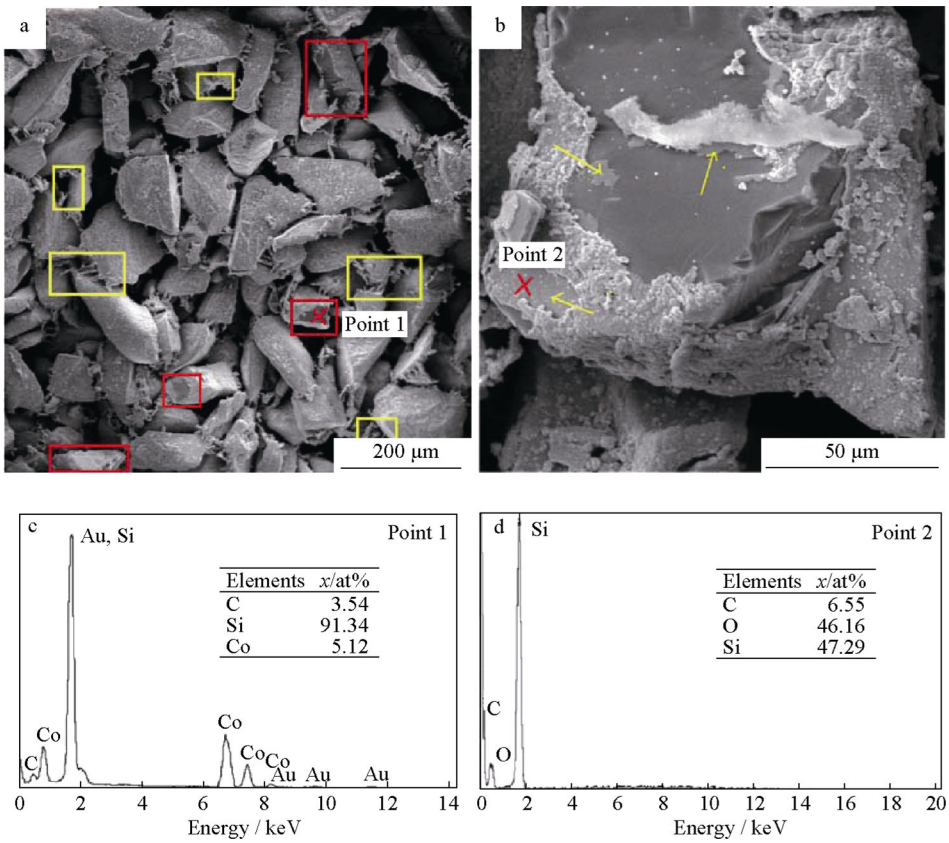

Fig. 9 SEM images **a**, **b** and corresponding EDS results **c**, **d** of Sample 28

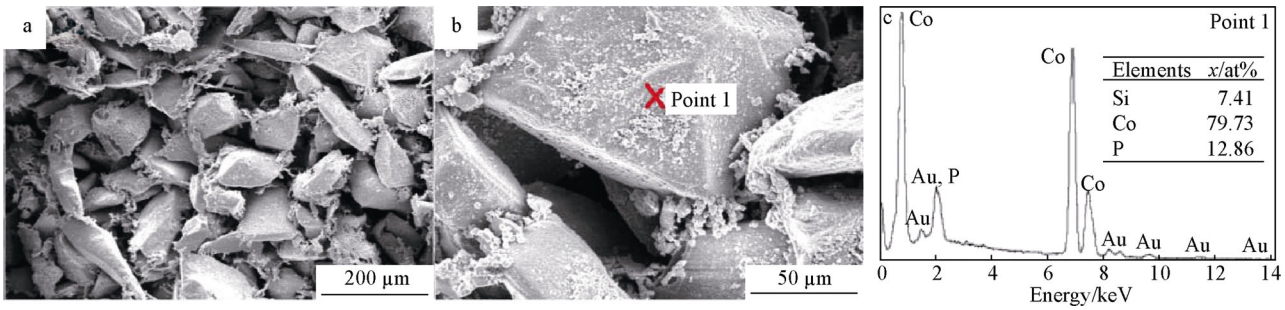

Fig. 10 SEM images and corresponding EDS result of Sample 26

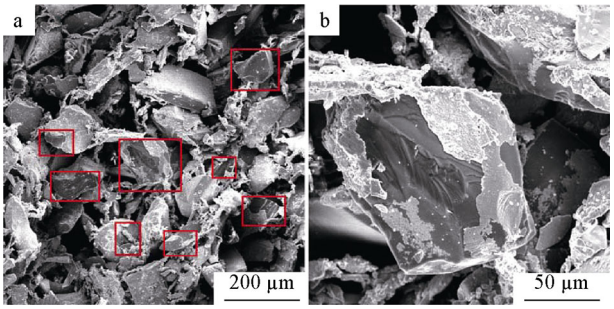

Fig. 11 SEM images of Sample 18 with different magnifications

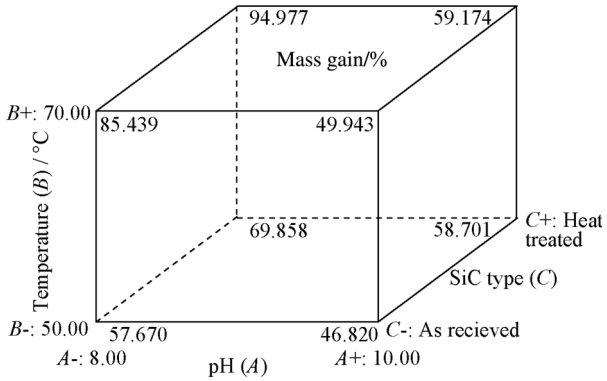

Fig. 12 Cube for response MG showing simultaneous effects of parameters

reducing agent. Equations (14) and (15) show these main reactions:

$$[CoXn]^{2+} + H_2PO_2^- + 3OH^- \rightarrow Co + HPO_3^{2-} + 2H_2O \quad (14)$$

$$H_2PO_2^- + OH^- \rightarrow 2[H] + HPO_3^{2-} \quad (15)$$

Equation (15) shows the consumption of hypophosphite during deposition, indicating that by increasing the deposition rate, the velocity of this reaction will also increase, leading to a decrease in MG of cobalt. In fact, the occurrence of the secondary reaction (Eq. (15)) would lead to a lower deposition of cobalt (Eq. (14)) as the necessary amount of $H_2PO_2^-$ will be consumed during this reaction (Eq. (15)). Based on the examinations, the deposition time for the heat-treated powders (around 134 min), which have a porous oxide layer in some parts, is considerably higher than that for as-received powders (around 117 min), and it is expected for heat-treated powders to have a higher amount of MG.

3.3 Optimization of parameters

The optimum parameters were selected using contour plots (Fig. 7), 3D plots (Fig. 7), cube plots (Fig. 12) and Table 2 in which the MG of the coatings is maximized. Accordingly, the results show that the maximum value of MG for the coatings that can be achieved during ED of SiC particles is 94.977 %. In addition, the process parameters for maximizing MG of the coatings are selected as 8, 70 °C and heat treatment for pH, bath temperature and SiC morphology, correspondingly.

4 Conclusion

Numerical models were effectively established to predict and optimize the MG of deposited cobalt on the SiC ceramic particles using RSM based on a full factorial design. Also, the ANOVA reveals that the models can be successfully applied for the prediction of MG. The most effective parameter for MG is pH. In addition, lower pH causes higher MG. With the temperature of ED bath increasing, MG of the deposited cobalt on the SiC particles increases. Moreover, the heat-treated SiC particles result in a higher MG in comparison with that of the as-received particles. SEM results indicate that pH makes a sharp change in MG and coating characteristics. In addition, it is concluded that the formation of a porous oxide layer on the ceramic particles after heating the powders affects MG. Finally, it is found that an increase in the bath temperature from 50 to 70 °C is useful and effective for cobalt coating. The highest value of 94.97 % for MG of the deposited

cobalt on the SiC particles is predicted by the developed mathematical model. Furthermore, the optimized pH, bath temperature and SiC particles morphology to get maximum amounts of MG are 8, 70 °C and heat-treated type, correspondingly.

References

[1] Valibeygloo N, Khosroshahi RA, Mousavian RT. Microstructural and mechanical properties of Al-4.5 wt% Cu reinforced with alumina nanoparticles by stir casting method. Int J Miner Metall Mater. 2013;20(10):978.

[2] Mohammadpour M, Khosroshahi RA, Mousavian RT, Brabazon D. Effect of interfacial-active elements addition on the incorporation of micron-sized SiC particles in molten pure aluminum. Ceram Int. 2014;40(6):8323.

[3] Mohammadpour M, Khosroshahi RA, Mousavian RT, Brabazon D. A novel method for incorporation of micron-sized SiC particles into molten pure aluminum utilizing a Co coating. Metall Mater Trans B. 2015;46(1):12.

[4] Roshan M, Mousavian RT, Ebrahimkhani H, Mosleh A. Fabrication of Al-based composites reinforced with Al_2O_3–TiB_2 ceramic composite particulates using vortex-casting method. J Min Metall Sect B. 2013;49(3):299.

[5] Rohatgi P. Cast aluminum-matrix composites for automotive applications. JOM. 1991;43(4):10.

[6] Boostani AF, Tahamtan S, Jiang ZY, Wei D, Yazdani S, Khosroshahi RA, Mousavian RT, Xu J, Zhang X, Gong D. Enhanced tensile properties of aluminium matrix composites reinforced with graphene encapsulated SiC nanoparticles. Compos A. 2015;68(2):155.

[7] Kaczmar J, Pietrzak K, Włosiński W. The production and application of metal matrix composite materials. J Mater Process Technol. 2000;106(1):58.

[8] Mousavian RT, Damadi SR, Khosroshahi RA, Brabazon D, Mohammadpour M. A comparison study of applying metallic coating on SiC particles for manufacturing of cast aluminum matrix composites. Int J Adv Manuf Technol. 2015. doi:10.1007/s00170-015-7246-4.

[9] Rawal SP. Metal-matrix composites for space applications. JOM. 2001;53(4):14.

[10] Emamy M, Nemati N, Heidarzadeh A. The influence of Cu rich intermetallic phases on the microstructure, hardness and tensile properties of Al–15% Mg_2Si composite. Mater Sci Eng A. 2010;527(12):2998.

[11] Heidarzadeh A, Emamy M, Rahimzadeh A, Soufi R, Heidary DSB, Nasibi S. The effect of copper addition on the fluidity and viscosity of an Al–Mg–Si alloy. J Mater Eng Perform. 2014;23(2):469.

[12] Hashim J, Looney L, Hashmi M. Metal matrix composites: production by the stir casting method. J Mater Process Technol. 1999;92–93:1.

[13] Hashim J, Looney L, Hashmi M. The enhancement of wettability of SiC particles in cast aluminium matrix composites. J Mater Process Technol. 2001;119(1):329.

[14] Hashim J, Looney L, Hashmi M. The wettability of SiC particles by molten aluminium alloy. J Mater Process Technol. 2001;119(1):324.

[15] Khosroshahi NB, Khosroshahi RA, Mousavian RT, Brabazon D. Effect of electroless coating parameters and ceramic particle size on fabrication of a uniform Ni–P coating on SiC particles. Ceram Int. 2014;40:12149.

[16] Khosroshahi NB, Khosroshahi RA, Mousavian RT, Brabazon D. Electroless deposition (ED) of copper coating on micron-sized SiC particles. Surf Eng. 2014;30(10):747.

[17] Zou G, Cao M, Lin H, Jin H, Kang Y, Chen Y. Nickel layer deposition on SiC nanoparticles by simple electroless plating and its dielectric behaviors. Powder Technol. 2006;168(2):84.

[18] Noori H, Mousavian RT, Khosroshahi RA, Brabazon D, Damadi SR. Effect of SiC particle morphology on Co–P electroless coating characteristics. Surf Eng. 2015. doi:10.1179/1743294415Y.0000000035.

[19] Deuis R, Subramanian C, Yellup J, Strafford K, Arora P. Study of electroless nickel plating of ceramic particles. Scr Metall Mater. 1995;33(8):1217.

[20] Wu Y, Li G, Zhang L. Wear resistance of electroless deposited Ni–P and Ni–P/SiC composite coatings on low alloy cast iron. Surf Eng. 2000;16(6):506.

[21] Luo L, Yu J, Luo J, Li J. Preparation and characterization of Ni-coated Cr_3C_2 powder by room temperature ultrasonic-assisted electroless plating. Ceram Int. 2010;36(6):1989.

[22] Mallory GO, Hajdu JB. Electroless Plating: Fundamentals and Applications. New York: Noyes Publication; 1990. 1.

[23] Abrantes L, Correia J. On the mechanism of electroless Ni–P plating. J Electrochem Soc. 1994;141(9):2356.

[24] Ohno I. Electrochemistry of electroless plating. Mater Sci Eng A. 1991;146(1):33.

[25] Box GEP, Wilson KB. On the experimental attainment of optimal conditions. J R Stat Soc. 1951;13:1.

[26] Box GEP, Hunter JS. Multi-factor experimental design for exploring response surfaces. Annal Math Stat. 1957;28:195.

[27] Farhanchi M, Neysari M, Barenji RV, Heidarzadeh A, Mousavian RT. Mechanical activation process for self-propagation high-temperature synthesis of ceramic-based composites. J Therm Anal Calorim. 2015. doi:10.1007/s10973-015-4704-z.

[28] Ilkhichi AR, Soufi R, Hussain G, Barenji RV, Heidarzadeh A. Establishing mathematical models to predict grain size and hardness of the friction stir-welded AA 7020 aluminum alloy joints. Metall Mater Trans B. 2015;46(1):357.

[29] Heidarzadeh A, Barenji RV, Esmaily M, Ilkhichi AR. Tensile properties of friction stir welds of AA 7020 aluminum alloy. Trans Indian Inst Metals. 2015. doi:10.1007/s12666-014-0508-2.

[30] Chang BP, Akil HM, Affendy MG, Khan A, Nasir RBM. Comparative study of wear performance of particulate and fiber-reinforced nano-ZnO/ultra-high molecular weight polyethylene hybrid composites using response surface methodology. Mater Des. 2014;63(2):805.

[31] Heidarzadeh A, Khodaverdizadeh H, Mahmoudi A, Nazari E. Tensile behavior of friction stir welded AA 6061-T4 aluminum alloy joints. Mater Des. 2012;37:166.

[32] Heidarzadeh A, Saeid T. Prediction of mechanical properties in friction stir welds of pure copper. Mater Des. 2013;52(24):1077.

[33] Kha TC, Nguyen MH, Roach PD, Stathopoulos CE. Microencapsulation of Gac oil: optimisation of spray drying conditions using response surface methodology. Powder Technol. 2014;264(3):298.

[34] Liu D, Huang C, Wang J, Zhu H, Yao P, Liu Z. Modeling and optimization of operating parameters for abrasive waterjet turning alumina ceramics using response surface methodology combined with Box–Behnken design. Ceram Int. 2014;40(6):7899.

[35] Rostamiyan Y, Fereidoon A, Mashhadzadeh AH, Ashtiyani MR, Salmankhani A. Using response surface methodology for modeling and optimizing tensile and impact strength properties of fiber orientated quaternary hybrid nano composite. Compos B Eng. 2015;69:304.

[36] Oraon B, Majumdar G, Ghosh B. Improving hardness of electroless Ni–B coatings using optimized deposition conditions and annealing. Mater Des. 2008;29(7):1412.

[37] Oraon B, Majumdar G, Ghosh B. Parametric optimization and prediction of electroless Ni–B deposition. Mater Des. 2007;28(7):2138.
[38] Poroch-Seritan M, Gutt S, Gutt G, Cretescu I, Cojocaru C, Severin T. Design of experiments for statistical modeling and multi-response optimization of nickel electroplating process. Chem Eng Res Des. 2011;89(2):136.
[39] Choudhury BS, Sen RS, Oraon B, Majumdar G. Statistical study of nickel and phosphorus contents in electroless Ni–P coatings. Surf Eng. 2009;25(5):410.
[40] Montgomery DC. Design and Analysis of Experiments. 5th ed. New York: Wiley; 2001. 239.
[41] Heidarzadeh A, Saeid T, Khodaverdizadeh H, Mahmoudi A, Nazari E. Establishing a mathematical model to predict the tensile strength of friction stir welded pure copper joints. Metall Mater Trans B. 2013;44(1):175.
[42] Jiang JT, Zhen L, Xu CY, Wu XL. Microstructure and magnetic properties of SiC/Co composite particles prepared by electroless plating. Surf Coat Technol. 2006;201(6):3139.